New era of asteroid-family studies:

with adaptive-optics observations of big asteroids

Miroslav Brož[1], P. Vernazza[2], L. Jorda[2], J. Hanuš[1],
M. Viikinkoski[3], M. Marsset[4], A. Drouard[2], R. Fetick[2], T. Fusco[2], B. Carry[5], F. Marchis[6],
M. Birlan, T. Santana-Ros, E. Jehin, and the HARISSA (High Angular Resolution Imaging Survey of the Shapes of Asteroids) team; D. Richardson, E. Asphaug, P. Ševecek[1]

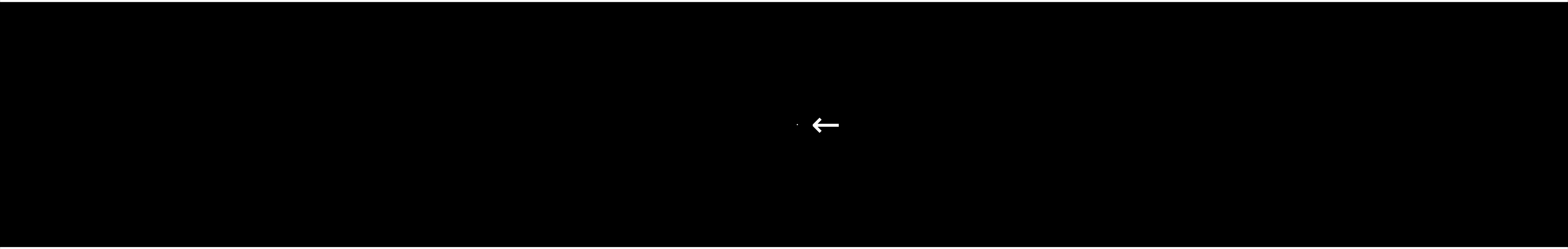

[1] Charles Univ in Prague, [2] Aix Marseille Univ, CNRS, LAM, [3] Tampere Univ, 4 Quenns Univ,
[5] Univ Cote d'Azur, [6] SETI Intitute, ...

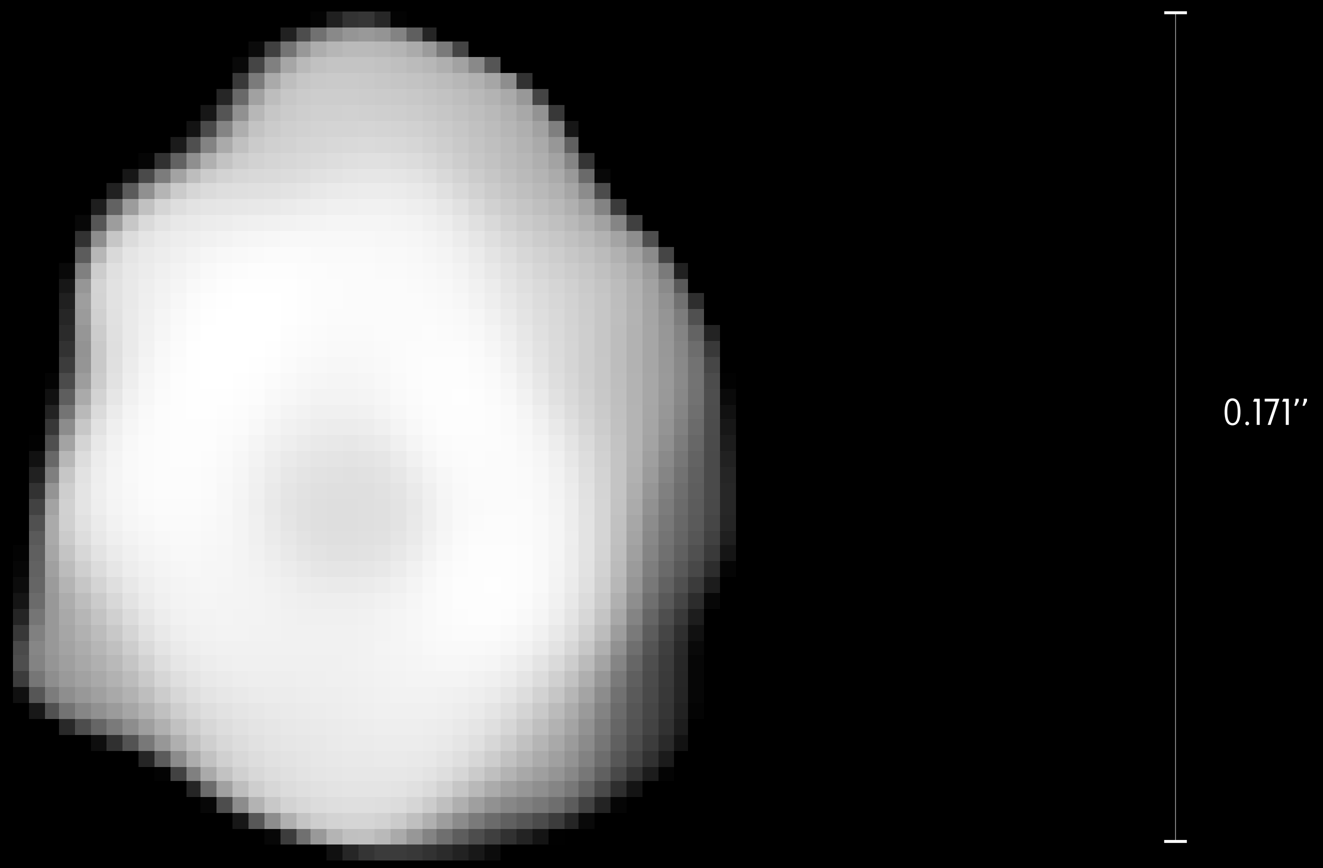
0.171''

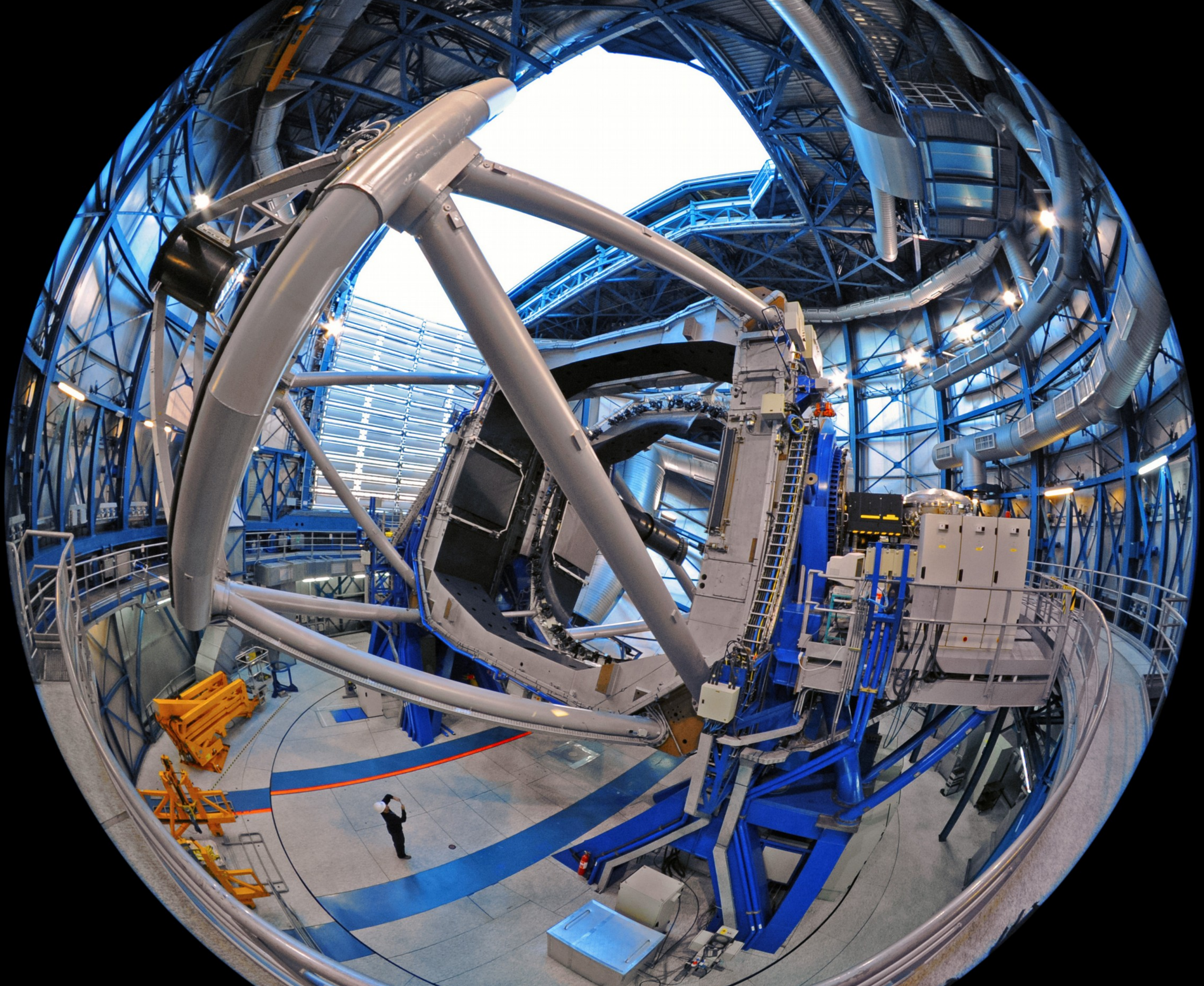

Extreme Adaptive Optics

$f = 1.2$ kHz, 40×40 lens & actuators ↑

- VLT/SPHERE/ZIMPOL instrument (Schmid etal. 2018), designed for exoplanets (M_J), diffraction-limited imaging, maximum contrast (planet/star), coronograph

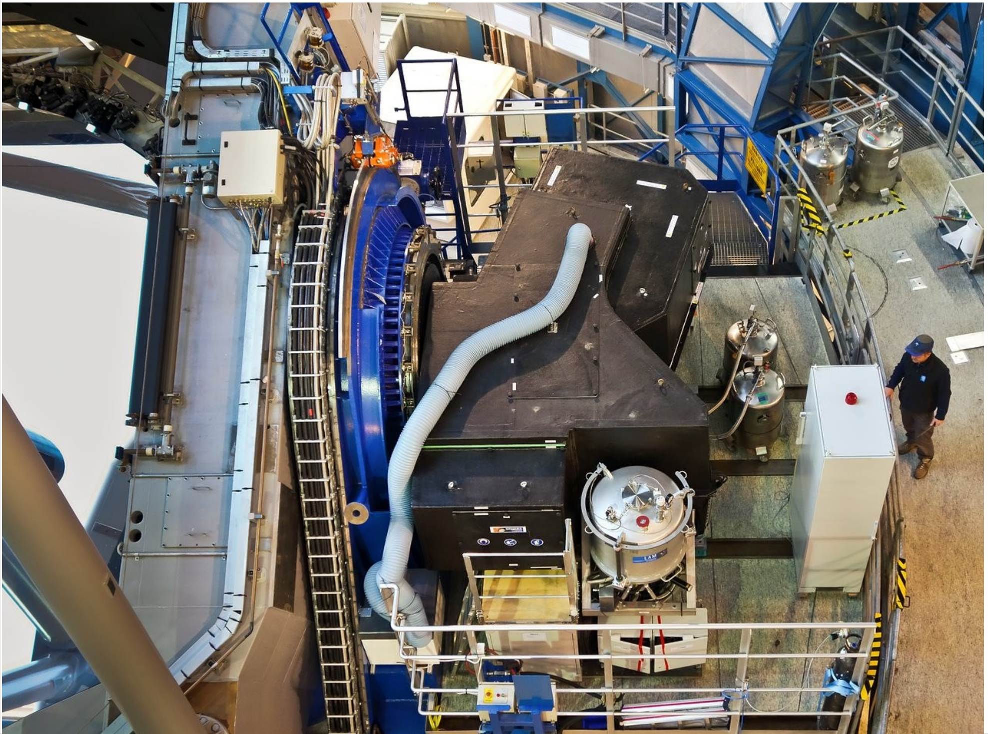

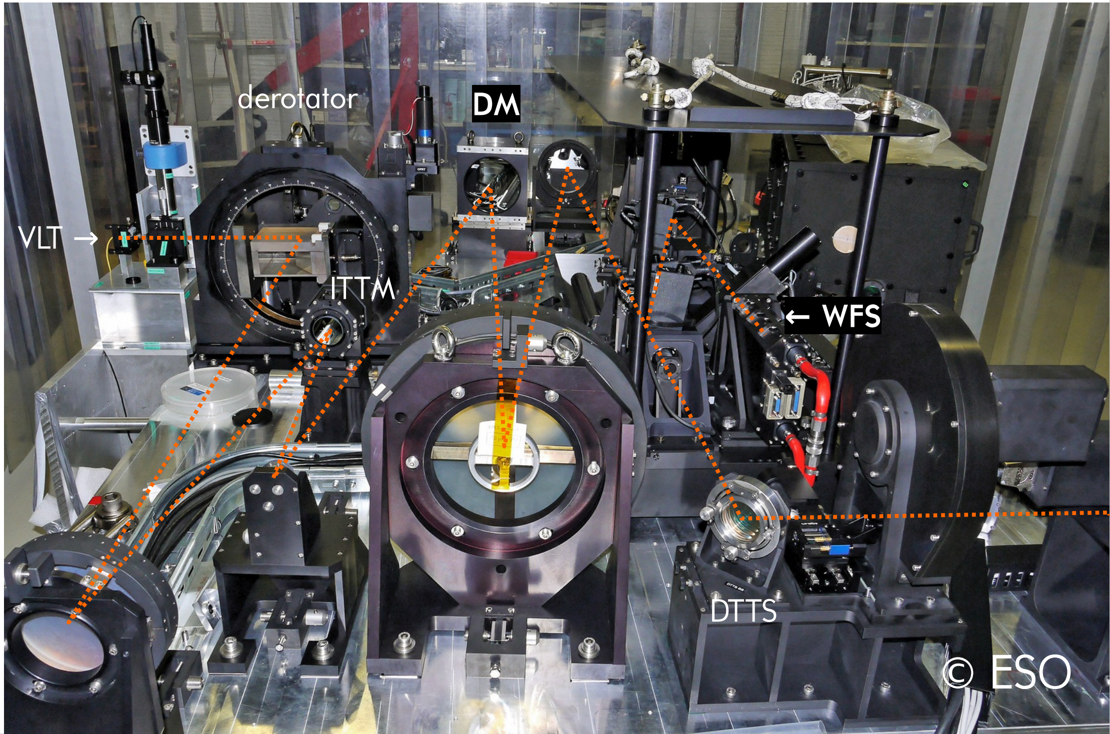

SPHERE instrument

- M1 tip-and-tilt → derotator → M2 → M3 tip-and-tilt → M4 → M5 deformable → M6 → M7 → M8 … M9 → M10 diff. tip-and-tilt → wavefront sensor …
- DM: 180 mm, 41×41 actuators, ±3.5 µm
- WFS: Hartmann-Shack, 40×40 lens, EMCCD, 6×6 pxl per sub-aperture
- NIR, V coronographs

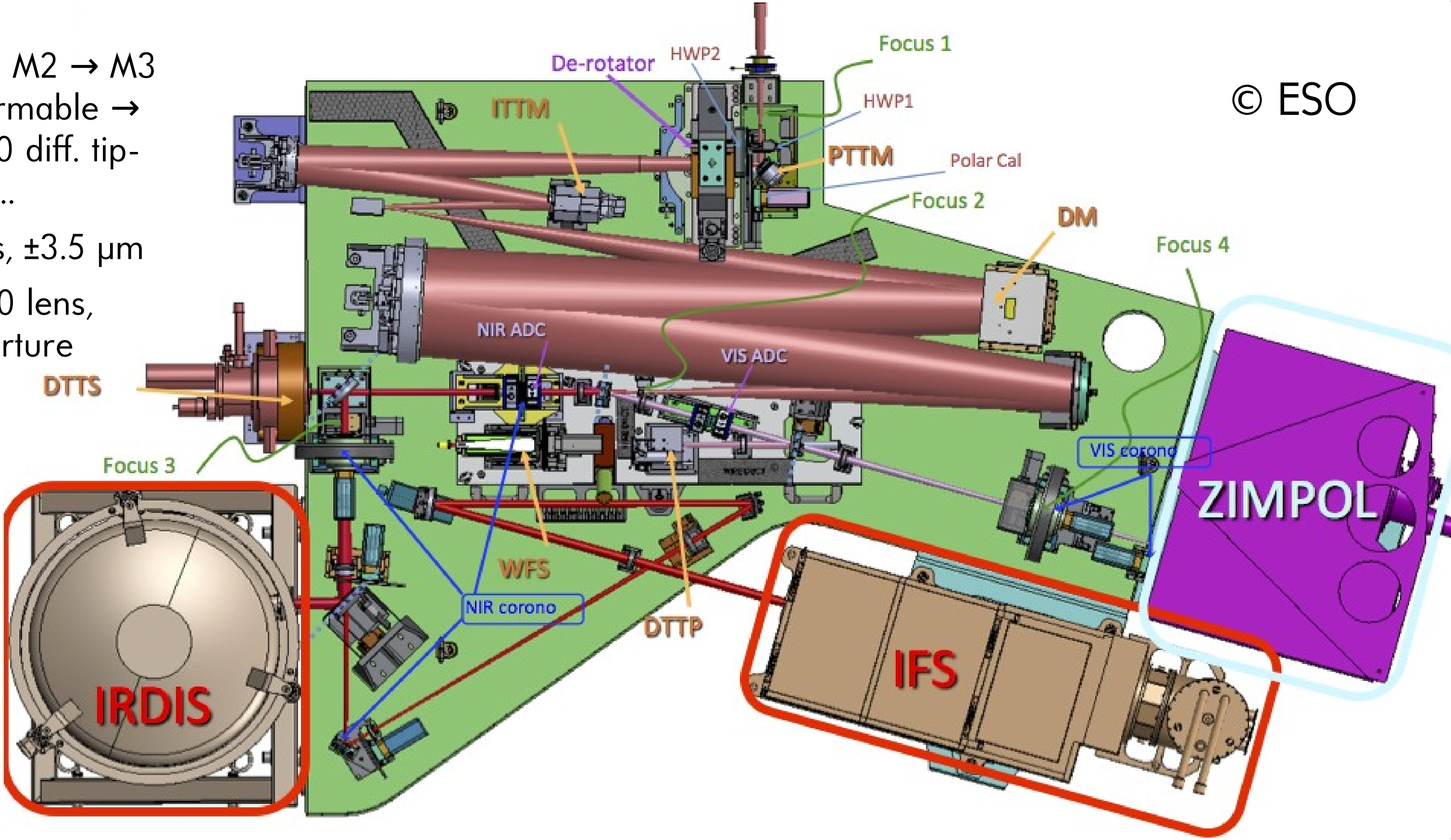

ZIMPOL instrument

- imaging polarimeter
- polarizer → electrooptic modulator (1 kHz) → polarizing beam splitter → filter wheels → M1's → M2's → cylindric lens → CCD's
- demodulation: 2nd rows masked, charges m. in/out
- for imaging only, Σ signals

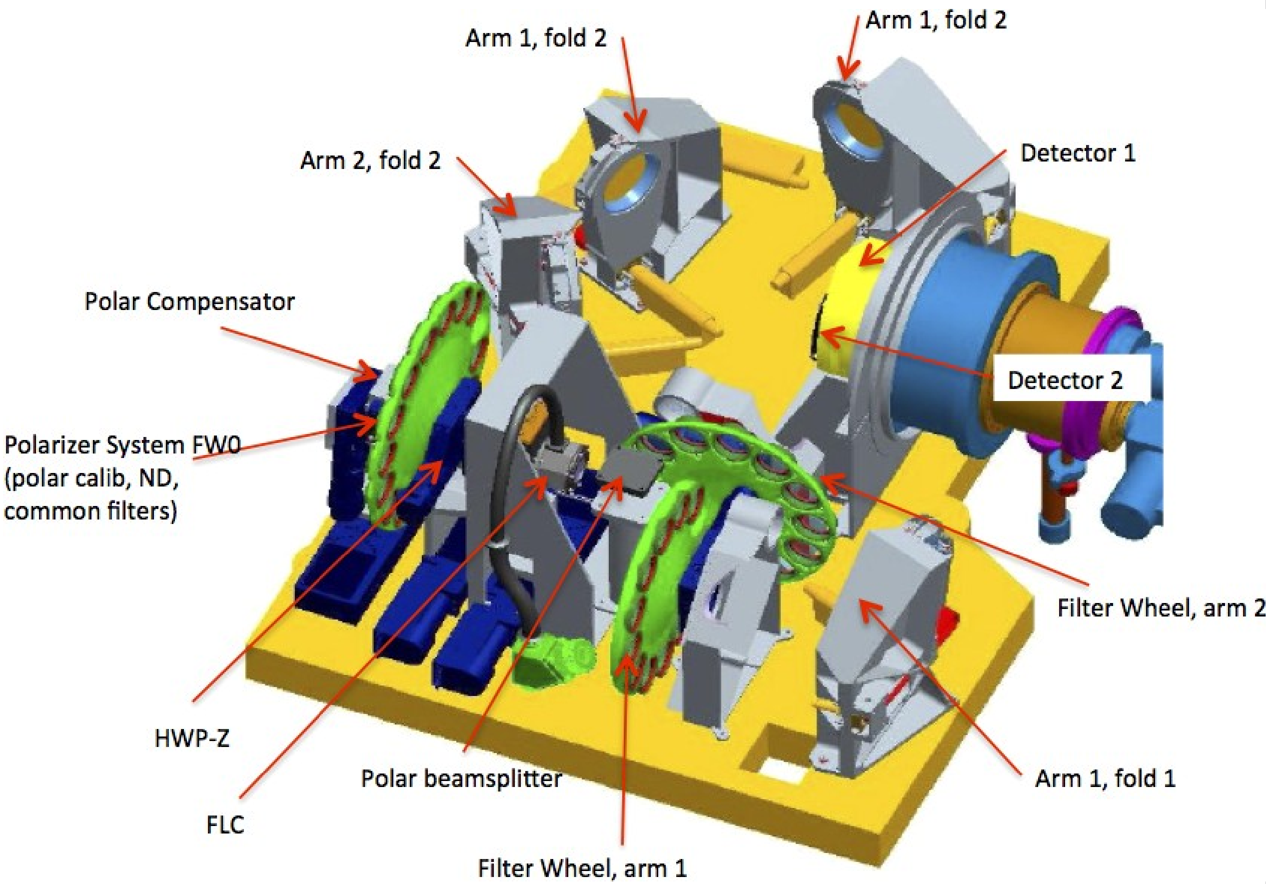

PSF & its variability

- N_R filter (645 ± 28 nm), dependence on λ, seeing conditions (<0.8'')
- asteroid as NGS, nearby * as PSF, 5 series of 10-s exposures @ epoch

1''

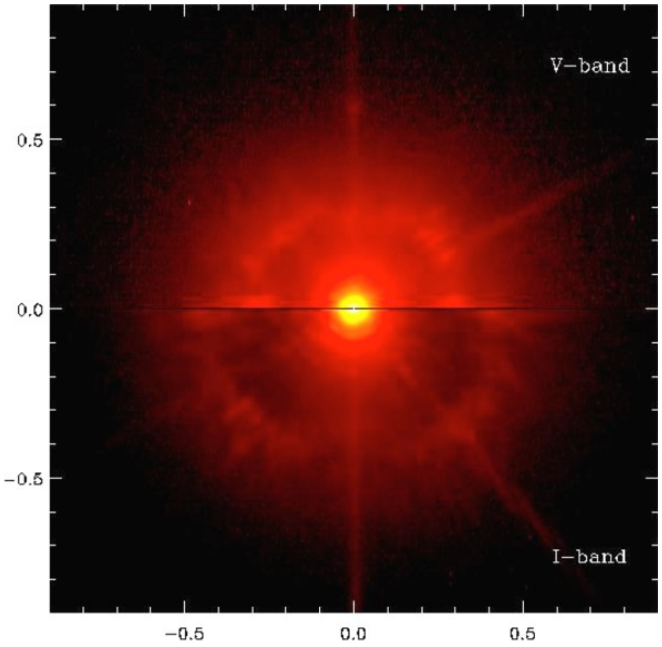

cf.

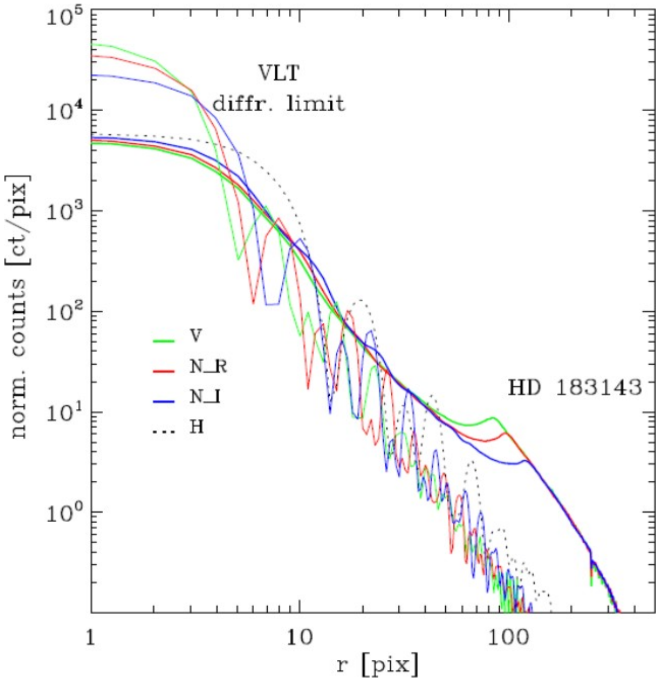

Schmid etal. (2017)

← Strehl 0.095 (V)

3.6 mas per pxl

Deconvolution (Bayes statistics)

- I ... degraded image, H ... PSF, O ... ideal image, N ... Noise

$$I = H * O + N$$

- Bayes theorem for conditional probabilities, where $p(I) = I \div 65535$ ADU

$$p(O \wedge I) = p(O|I)p(I) = p(I|O)p(O) \;\rightarrow\; p(O|I) = \frac{p(I|O)p(O)}{p(I)}$$

- maximalisation of $p(O|I)$, i.e. minimalisation of the functional wrt. O:

$$J = -\ln[p(I|O)p(O)] = -\ln p(I|O) - \ln p(O) \equiv J_N + J_O$$

Deconvolution (Richardson-Lucy)

- Poisson statistics for $p(I\,|O)$, where k … I, λ … $H*O$ & functional:

$$p(k;\lambda) = \frac{\lambda^k\, \mathrm{e}^{-\lambda}}{k!}$$

$$J_N = -\ln p(I|O) = \sum_r [-I \ln(H*O) + H*O]$$

- min: compute ∇, shift to $-\nabla$, in case of convergence ($n \to \infty$) assume $O^{n+1} = O^n$ → iterative algorithm (Richardson 1972, Lucy 1974):

$$O^{n+1}(r) = O^n(r) \left[H(-r) * \frac{I(r)}{H(r) * O^n(r)} \right]$$

Myopic deconvolution ← MISTRAL algorithm

- problems of RL: divergence (if not P.), artifacts on edges, "ringing"
- Gaussian noise (photon, PSF, seeing, jitter, ...), regularisation (Conan etal. 2000):

$$p(x;\sigma) = \frac{1}{\sigma\sqrt{2\pi}} \mathrm{e}^{-\frac{x^2}{2\sigma^2}} \quad \rightarrow \quad J_N = \sum_r \frac{1}{2\sigma^2} (I - H * O)^2$$

- additional priors (edge, seeing), 2nd regularisation:

$$J_O = -\ln p(O) = \mu \sum_r \left[\frac{|\nabla O|}{\delta} - \ln\left(1 + \frac{|\nabla O|}{\delta}\right)\right]$$

$$J_H = \frac{1}{2} \sum_q \frac{|\tilde{H} - \mathrm{E}(\tilde{H})|^2}{\mathrm{E}[|\tilde{H} - \mathrm{E}(\tilde{H})|^2]}$$

δ, μ ... free parameters,
E() ... expectation (average over I),
$\tilde{H}$ ... Fourier transform, i.e. MTF

degraded image

=

stellar PSF

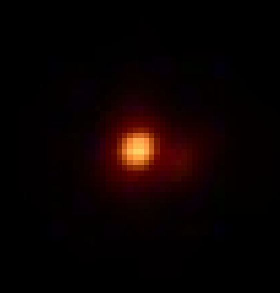

*

deconvolved image

8 epochs
Jul 7th - Oct 10th 2017
mypoic deconvolution
by MISTRAL algorithm
(Fusco etal. 2003)

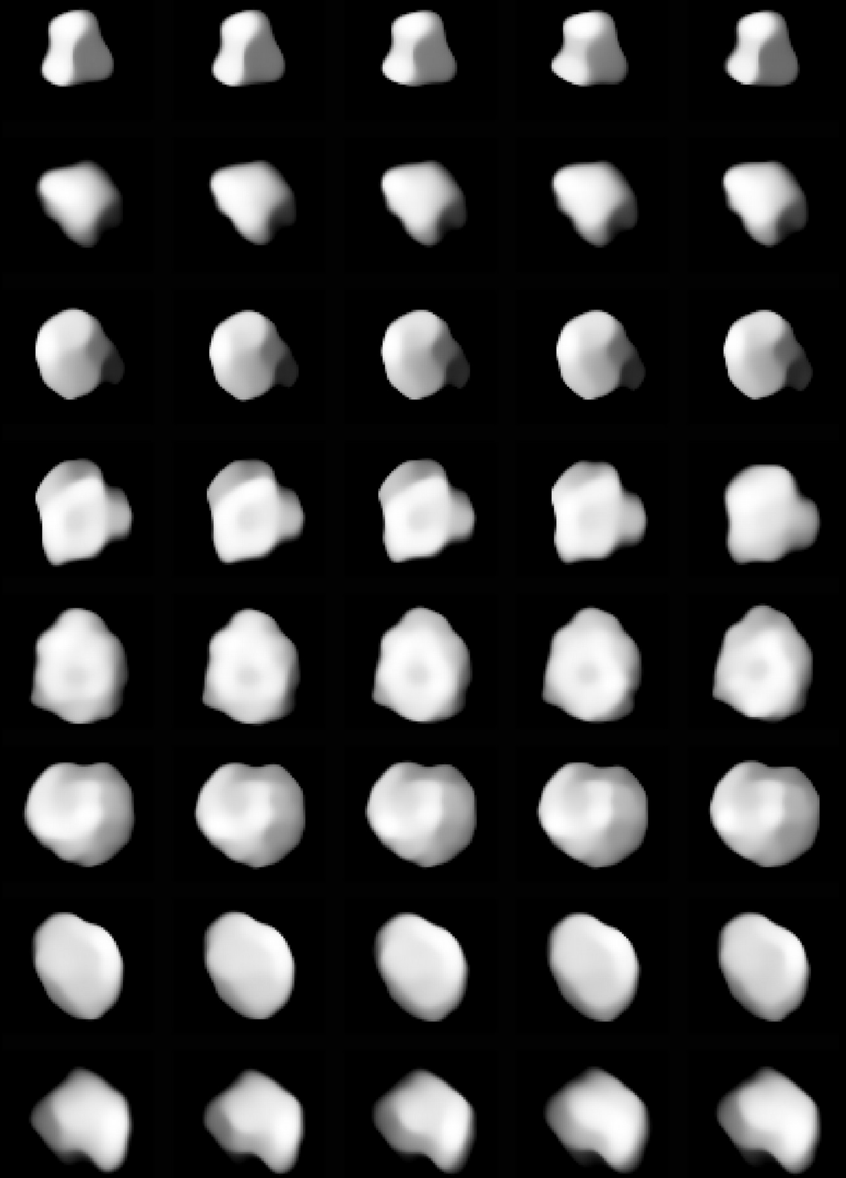

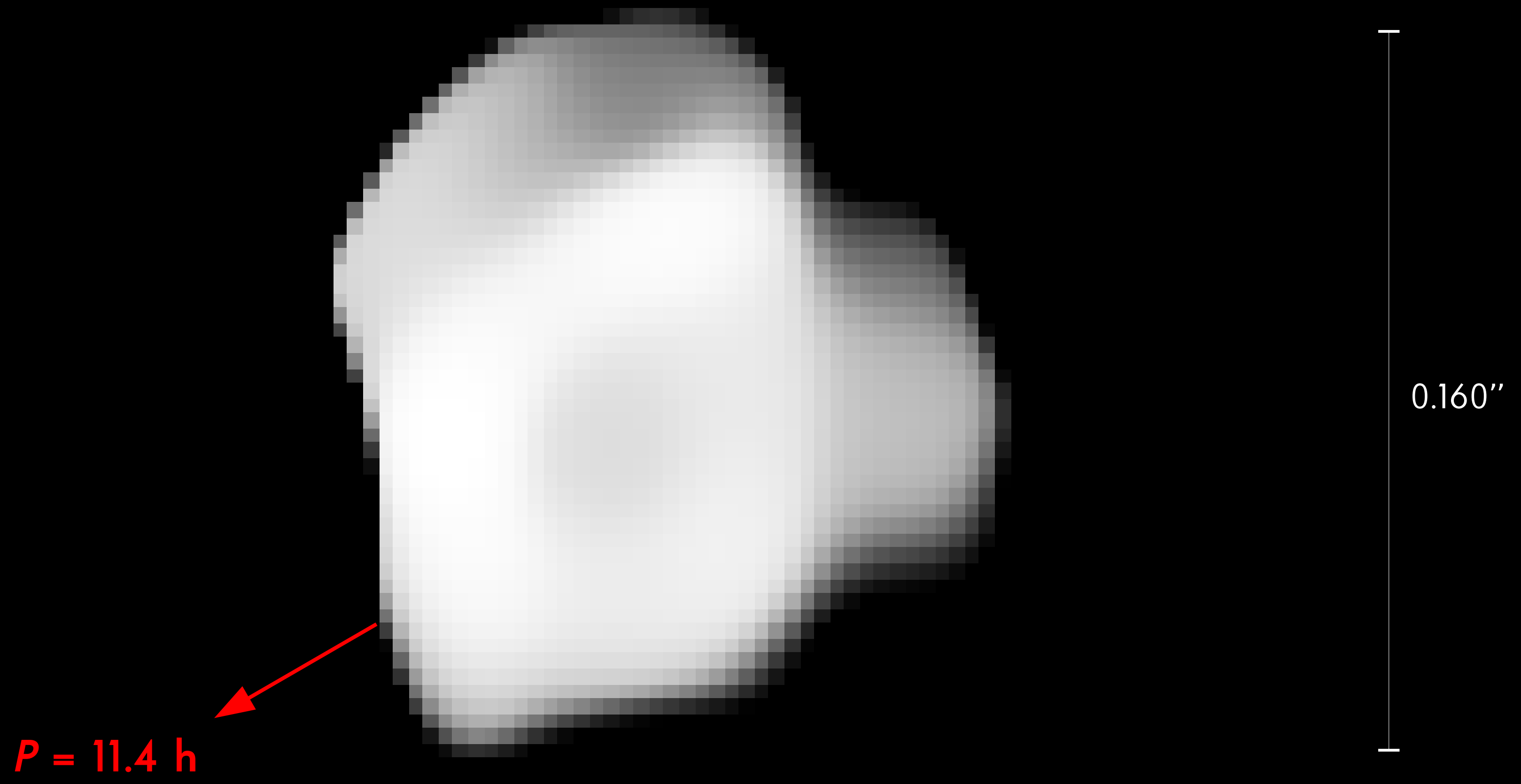
0.160″
P = 11.4 h

Crater ("Nonza")

- 3D shape reconstruction by ADAM (Viikinkoski etal. 2015): AO + LC + regularisation
- crater visible at longitude 0° (def.) and latitude -32°

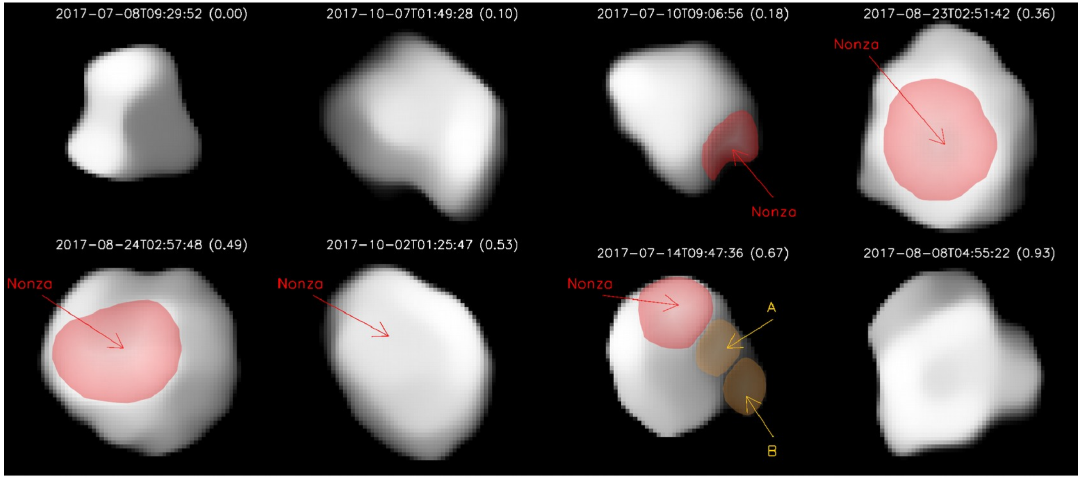

Fig. 3: Identification of the impact craters present at the surface of Julia. Besides the large impact basin Nonza, we identified two possible small craters (A and B) at rotational phase 0.67.

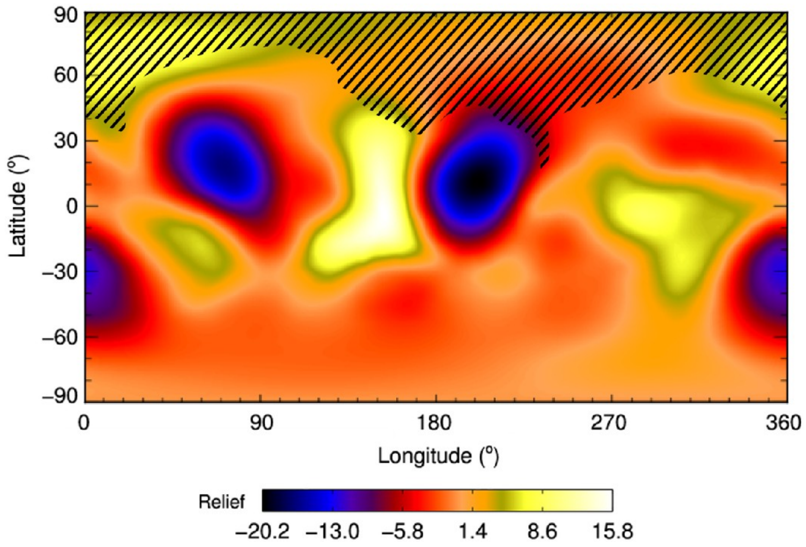

Main Asteroid Belt

- synthetic proper elements (Kneževic & Milani 2003)
- WISE albedos (Masiero etal. 2014)
- **125** families (Nesvorný etal. 2015)

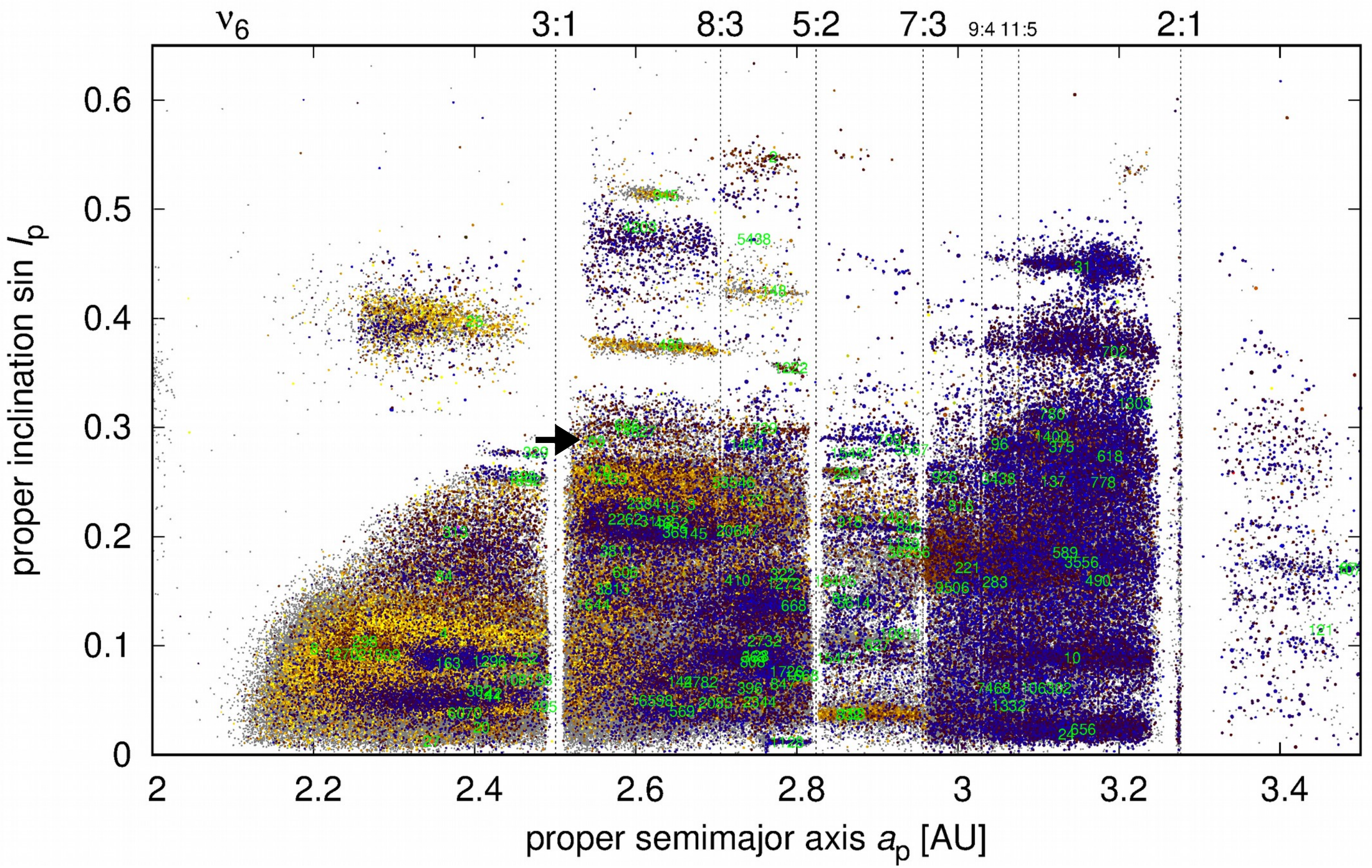

Julia family identification

- middle belt, high-I, low # of a. (Nesvorný etal. 2015)
- hierarchical clustering (Zappala etal. 1995) with $v_{\rm cut}$ = 80 m/s → 66 members
- taxonomy **S** (or K?)
- albedo $p_V = 0.184$
- **LL chondrites** analogue (Vernazza etal. 2014) → $\rho_{\rm bulk}$ = 3300 kg/m^3

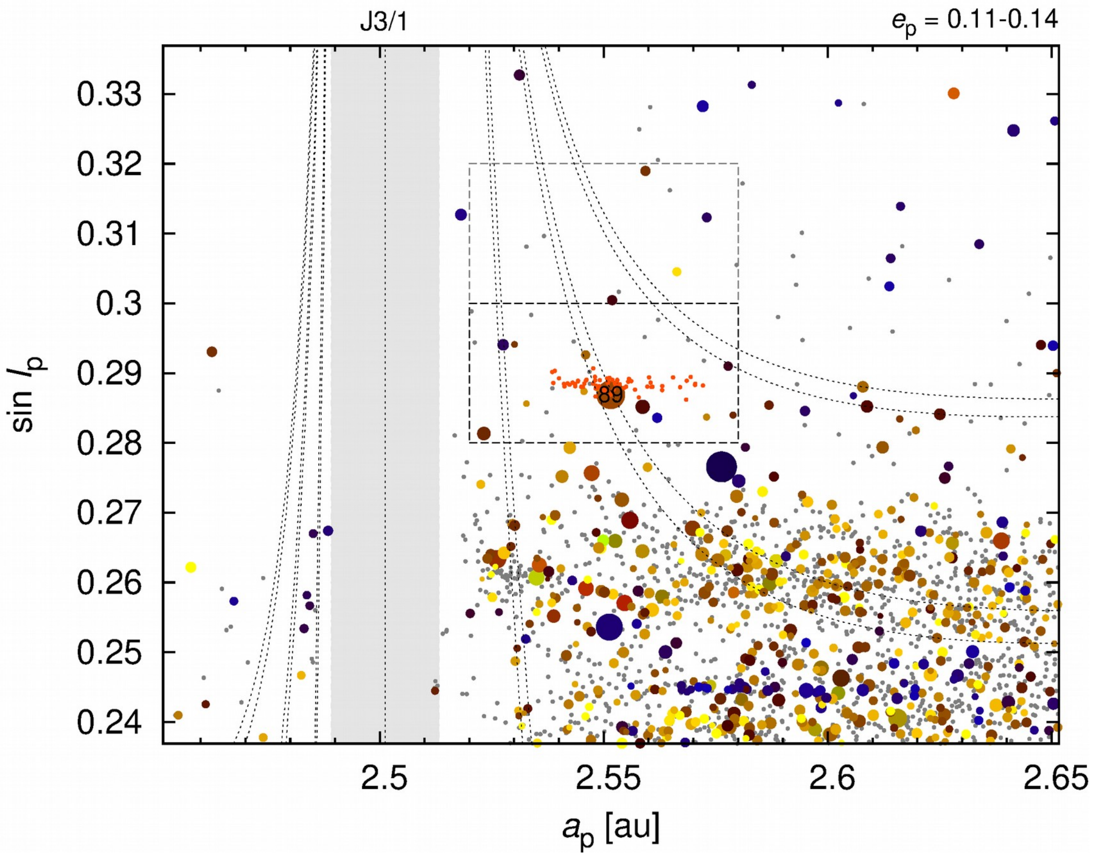

0. Preliminary analysis

- **escape velocity** $v_{esc} \doteq 115$ m/s
- ellipses due to **Gauss equations**:

$$\Delta a = \frac{2}{n\sqrt{1-e^2}}[\Delta v_T + e(\Delta v_T \cos f + \Delta v_R \sin f)]$$

$$\Delta e = \frac{\sqrt{1-e^2}}{na}[\Delta v_R \sin f + \Delta v_T(\cos f + \cos E)]$$

- a cut at $a_p = 2.54$ au ← proximity to J3/1 or secular resonances?
- a shift in $\Delta I_p = 0.002$ rad ← ejection into half-space?

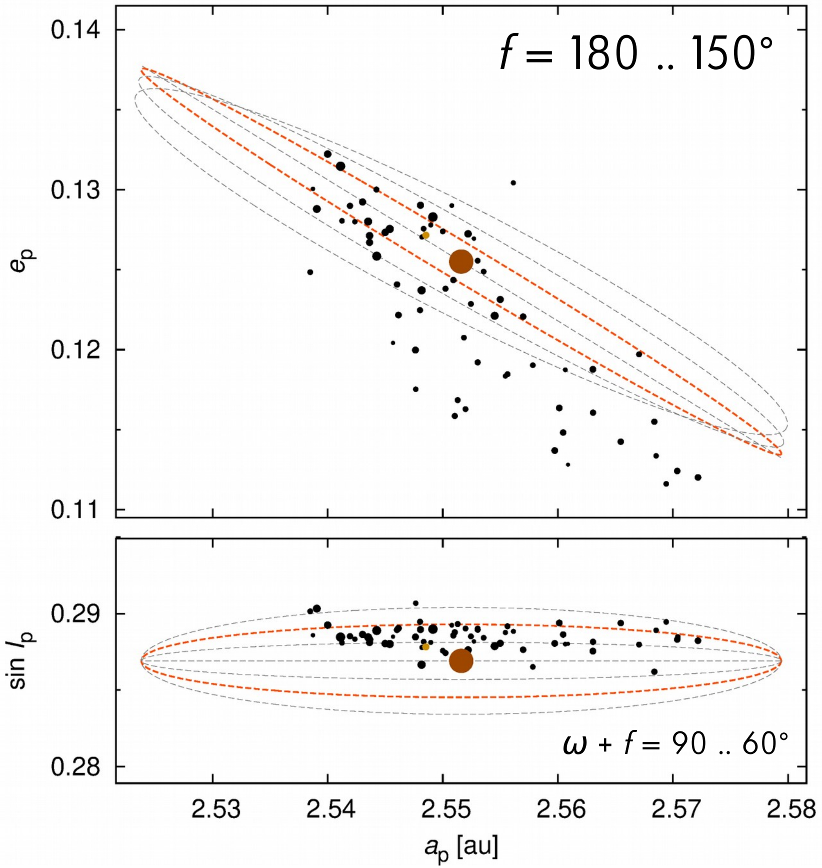

1. N-body orbital simulation

We use a symplectic integration scheme (Levison and Duncan 1994), denoted as kick–drift–kick, where the 'kick' (actually, a perturbation) is performed as:

$$\dot{\mathbf{r}}_{n+1} = \dot{\mathbf{r}}_n + \ddot{\mathbf{r}}\frac{\Delta t}{2}\,, \tag{3}$$

and the 'drift' corresponds to an analytical solution of the two-body problem (the Sun–asteroid), which involves a numerical solution of the transcendent Kepler equation:

$$\begin{aligned} M &= E - e\sin E\,, && (4)\\ \mathbf{r}_{n+1} &= p(E)\mathbf{r}_n + q(E)\dot{\mathbf{r}}_n\,, && (5)\\ \dot{\mathbf{r}}_{n+1} &= \dot{p}(E)\mathbf{r}_n + \dot{q}(E)\dot{\mathbf{r}}_n\,; && (6) \end{aligned}$$

we account for gravitational perturbations by planets, expressed in the heliocentric frame:

$$\ddot{\mathbf{r}}_j = \sum_i \left[-\frac{Gm_i}{r_i^3}\mathbf{r}_i - \frac{Gm_i}{r_{ji}^3}\mathbf{r}_{ji}\right]\,, \tag{7}$$

possibly, the planetary migration, in an analytical way (Malhotra 1995), and also eccentricity damping (Morbidelli et al. 2010):

$$\dot{\mathbf{r}}_{n+1} = \dot{\mathbf{r}}_n\left[1 + \frac{\Delta v}{\dot{r}}\frac{\Delta t}{\tau_{\mathrm{mig}}}\exp\left(-\frac{t-t_0}{\tau_{\mathrm{mig}}}\right)\right]\,, \tag{8}$$

the Yarkovsky thermal effect (Vokrouhlický 1998, Vokrouhlický and Farinella 1999):

$$
\begin{aligned}
f_X(\zeta) + \mathrm{i} f_Y(\zeta) &= -\frac{8}{3\sqrt{3\pi}}\, \Phi\, t'_{1-1}(R';\zeta)\,, && (9)\\
f_Z(\zeta) &= -\frac{4}{3}\sqrt{\frac{2}{3\pi}}\, \Phi\, t'_{10}(R';\zeta)\,, && (10)\\
\Phi &\equiv \frac{(1-A)\mathcal{E}_\star \pi R^2}{m_j c_{\mathrm{vac}}}\,, && (11)
\end{aligned}
$$

the YORP effect (Čapek and Vokrouhlický 2004):

$$
\begin{aligned}
\dot{\omega} &= c f_k(\gamma)\,, && (12)\\
\dot{\gamma} &= \frac{c g_k(\gamma)}{\omega}\,, && (13)\\
c &\equiv c_{\mathrm{YORP}} \left(\frac{a}{a_0}\right)^{-2} \left(\frac{R}{R_0}\right)^{-2} \left(\frac{\rho}{\rho_0}\right)^{-1}, && (14)
\end{aligned}
$$

mass shedding beyond the critical angular frequency (Pravec and Harris 2000):

$$
\omega_{\mathrm{crit}} = \sqrt{\frac{4}{3}\pi G \rho}\,, \tag{15}
$$

and random collisional reorientations with the time scale (Farinella et al. 1998):

$$
\tau_{\mathrm{reor}} = B \left(\frac{\omega}{\omega_0}\right)^{\beta_1} \left(\frac{R}{R_0}\right)^{\beta_2}. \tag{16}
$$

N-body (cont.)

- dynamical model: Sun + 4 giant planets + (13) Egeria (Levison & Duncan 1994), Yarkovsky diurnal & seasonal effect (Vokrouhlický 1998), YORP effect (Čapek & Vokrouhlický 2004), collisional reorientations, mass shedding @ ω_{crit}
- 660 particles, v_{max} = 500 m/s, ρ_{surf} = 1500 kg/m^3, $K = 10^{-3}$ W/m/K, …

“0 Myr” 30 Myr 520 Myr

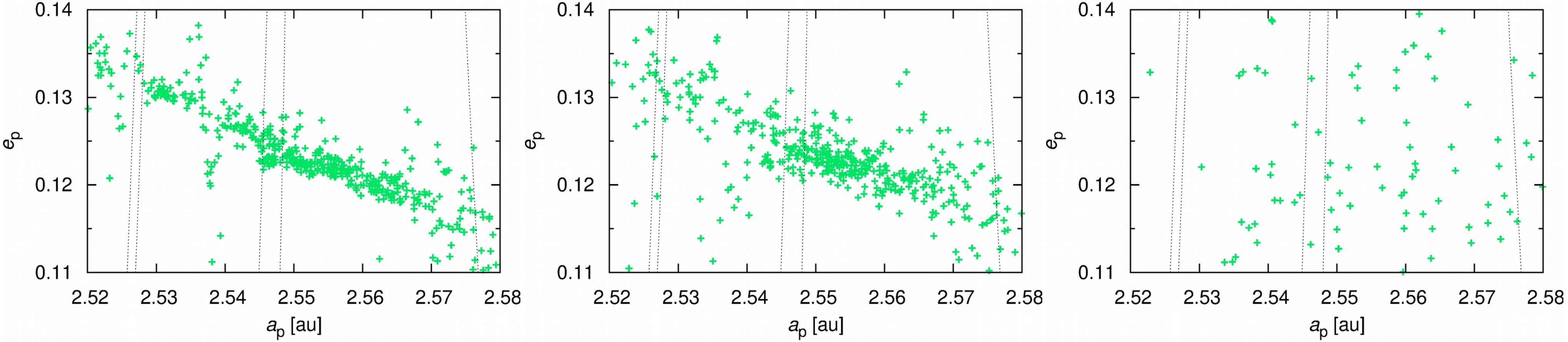

N-body (cont.)

- post-processing: (i) uniform background, (ii) match **SFD** @ every time step, (iii) random selection of orbits from ICs (see Brož & Morbidelli 2018)
- sorry for being so noisy, but 66 is low number…
- Julia family **age**: 10 to 120 Myr (i.e. both lower and upper limits)

“0 Myr”

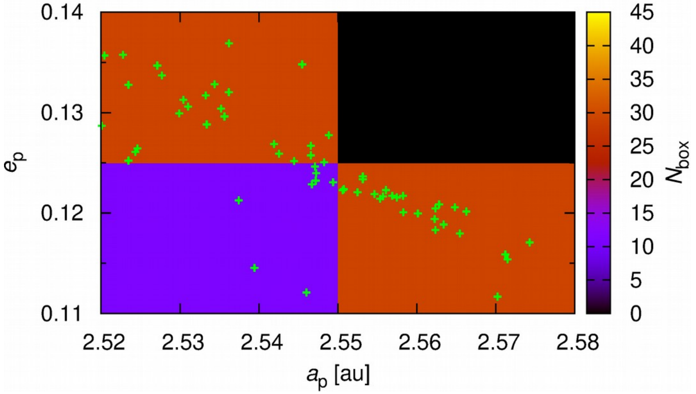

30 Myr

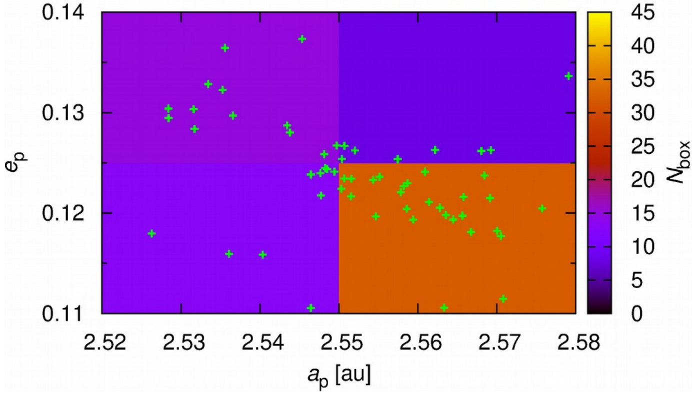

~~520 Myr~~

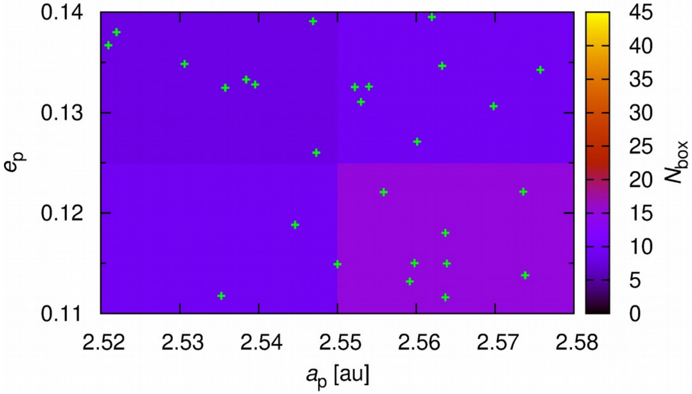

Comparison of simulations & observations

- # of a. in boxes in (a_p, e_p) space
- suitable χ^2 metric (Poissonian σ):

$$\chi^2 = \sum_{i=1}^{N_{\mathrm{box}}} \frac{(N_{\mathrm{syn}\,i} - N_{\mathrm{obs}\,i})^2}{\sigma^2_{\mathrm{syn}\,i} + \sigma^2_{\mathrm{obs}\,i}}$$

observed

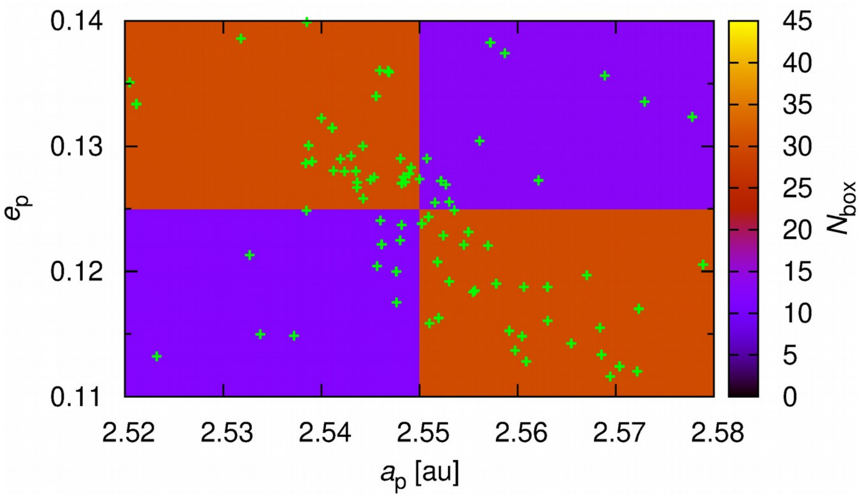

age

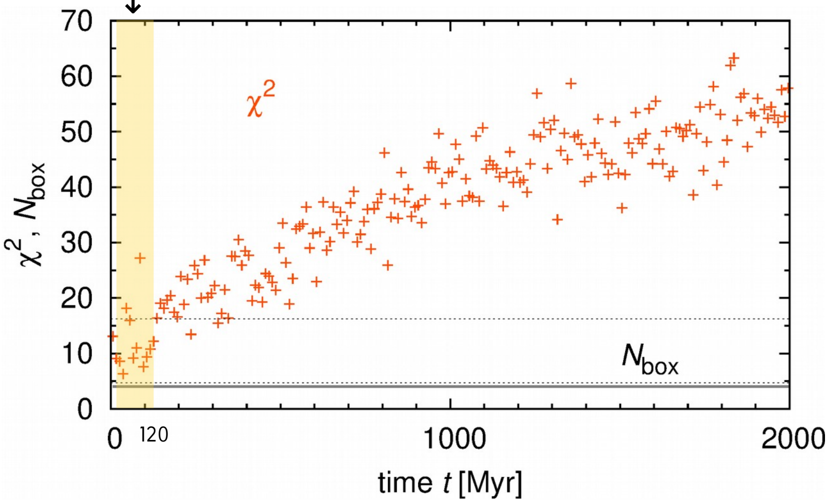

2. SPH break-up simulation

- fragmentation by SPH5 (Benz & Asphaug 1994), reaccumulation by Pkdgrav (Richardson etal. 2000)
- Tillotson (1962) EOS, von Mises yielding, Grady & Kipp (1980) fracture model, no porosity
- basalt material with ρ_0 = 3300 kg/m^3
- $N = 1.4 \cdot 10^6$ to resolve LF
- **IC**: d = 8 km, v = 6 km/s, θ = 75°, …
  → fragment SFD, v-field, **crater size**

↑
transient

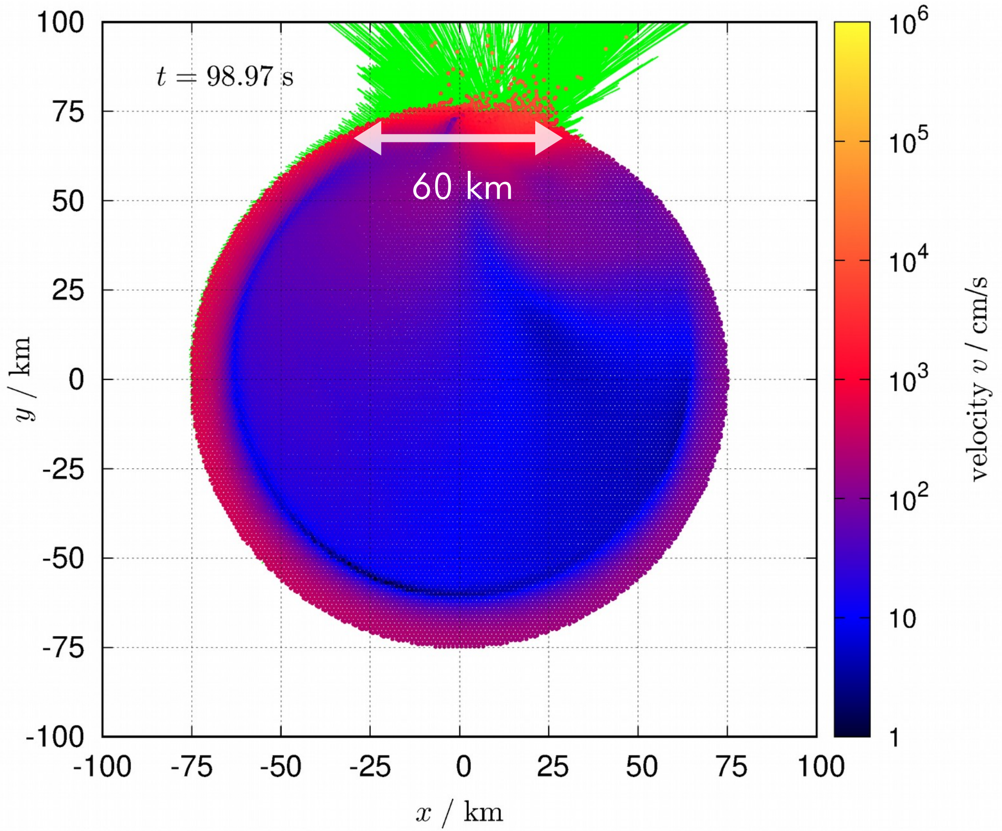

SPH (cont.)

- size-frequency distribution $N\,(>D)$ → barely resolved **LF** (slope unreliable)
- correction of M_{LF}/M_{tot} parametric relation from Morbidelli etal. (2009) ← important!

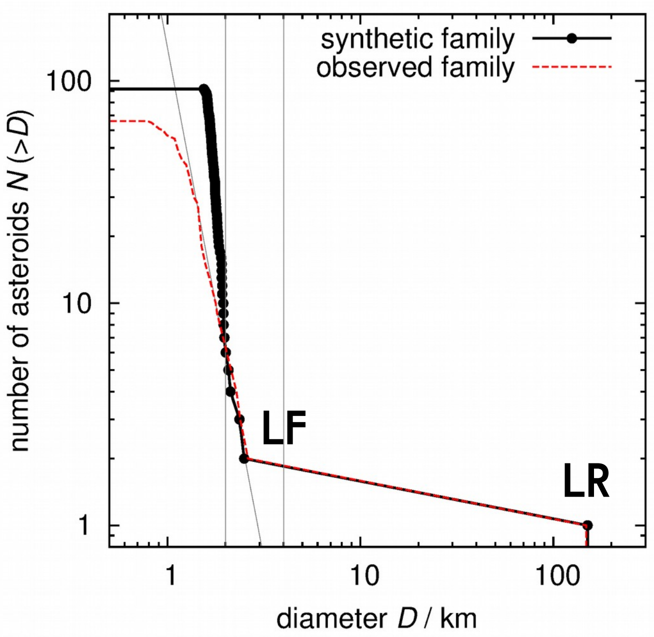

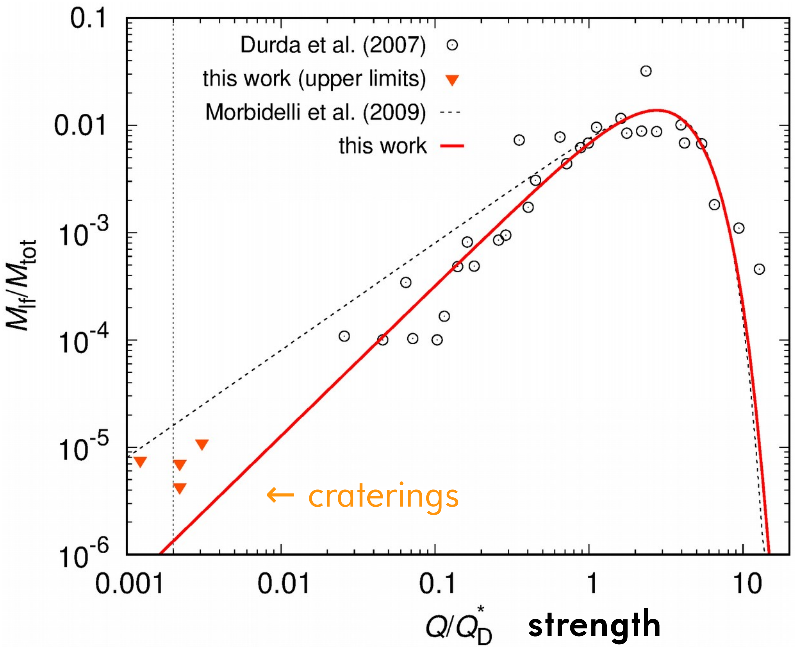

SPH (cont.)

- **IC**: d = 4.4 km, v = 6 km/s, θ = 15°
- not a unique solution...

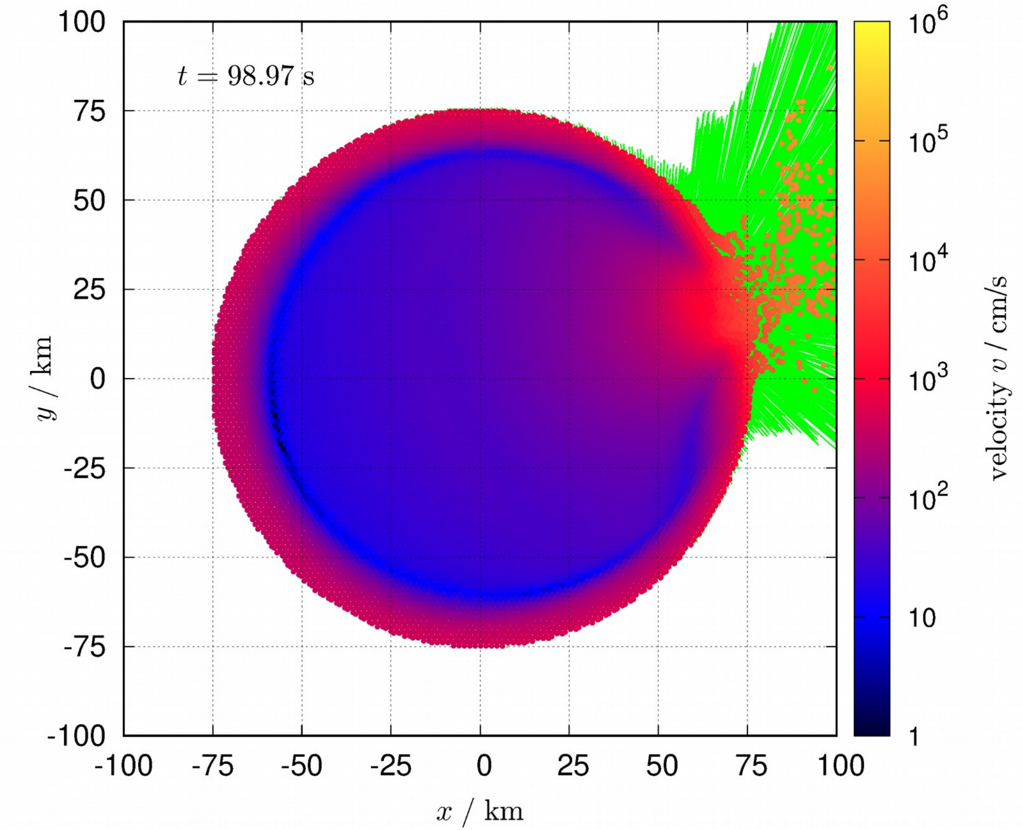

3. Monte-Carlo collisional models

(e.g. Boulder code, Morbidelli et al. 2009)

- Monte-Carlo approach
- number of disruptions
- parametric relations (from SPH)
- largest remnant
- largest fragment
- SFD slope of fragments
- dynamical decay

pseudo-random-number generator for rare collisions

specific energy $Q = ½\, m_i v^2/M_{\rm tot}$, $Q_{\rm D}$ … scaling law

focussing

$$n_{ij} = p_{\rm i}(t) f_{\rm g} \frac{(D_i + d_j)^2}{4} n_i n_j \Delta t$$

$$M_{\rm LR} = \left[-\frac{1}{2}\left(\frac{Q}{Q_D^\star} - 1\right) + \frac{1}{2}\right] M_{\rm tot} \quad \text{for } Q < Q_D^\star$$

$$M_{\rm LR} = \left[-0.35\left(\frac{Q}{Q_D^\star} - 1\right) + \frac{1}{2}\right] M_{\rm tot} \quad \text{for } Q > Q_D^\star$$

$$M_{\rm LF} = 8 \times 10^{-3} \left[\frac{Q}{Q_D^\star} \exp\left(-\left(\frac{Q}{4Q_D^\star}\right)^2\right)\right] M_{\rm tot}$$

$$q = -10 + 7\left(\frac{Q}{Q_D^\star}\right)^{0.4} \exp\left(-\frac{Q}{7Q_D^\star}\right)$$

Monte-Carlo (cont.)

- Boulder code (Morbidelli etal. 2009), scaling law of Benz & Asphaug (1999), ...
- without (89) Julia (LR), i.e. only fragments → family lifetime ~ 100 Myr

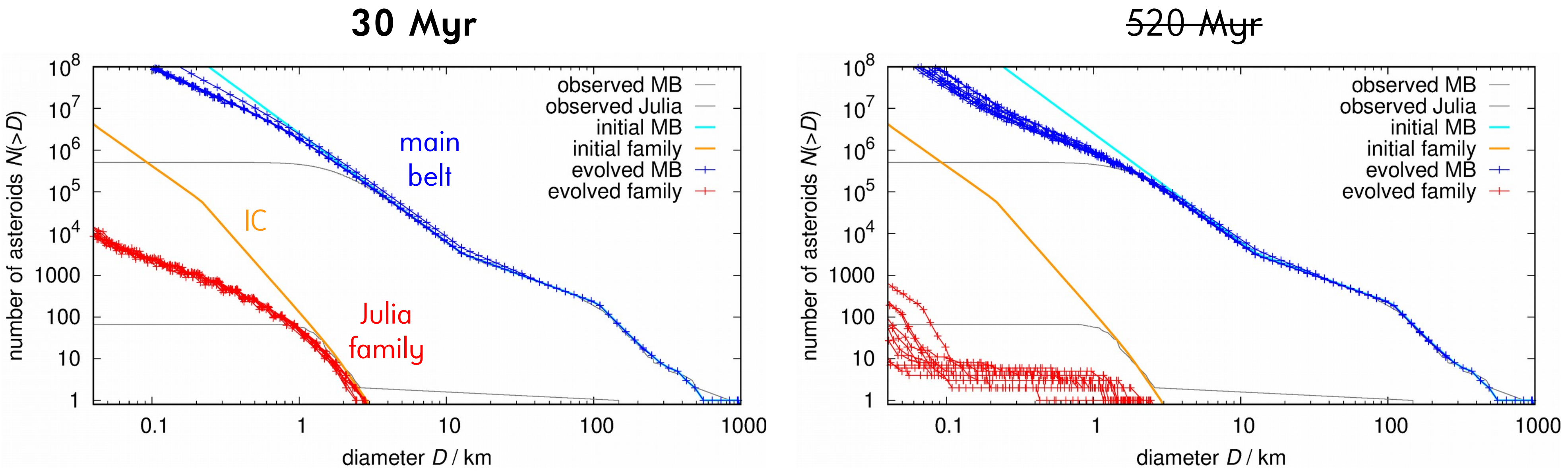

Monte-Carlo (cont.)

$D_{LF} \geq 2.6$ km

- the same with (89) Julia → number of events: **1 to 10** per 4 Gyr (100 MC runs)
- if ≫ 1 then possible **resurfacing**? irregular shape?

30 Myr

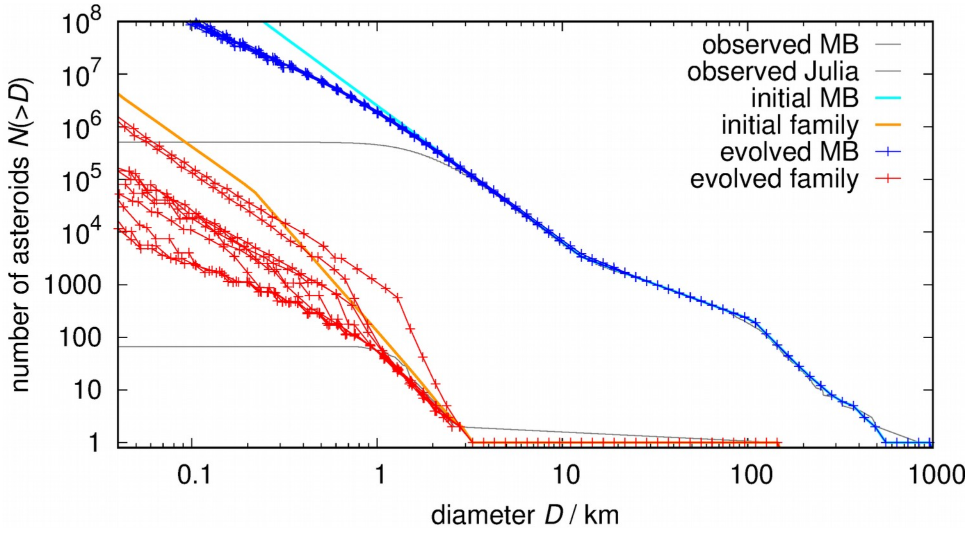

~~520 Myr~~

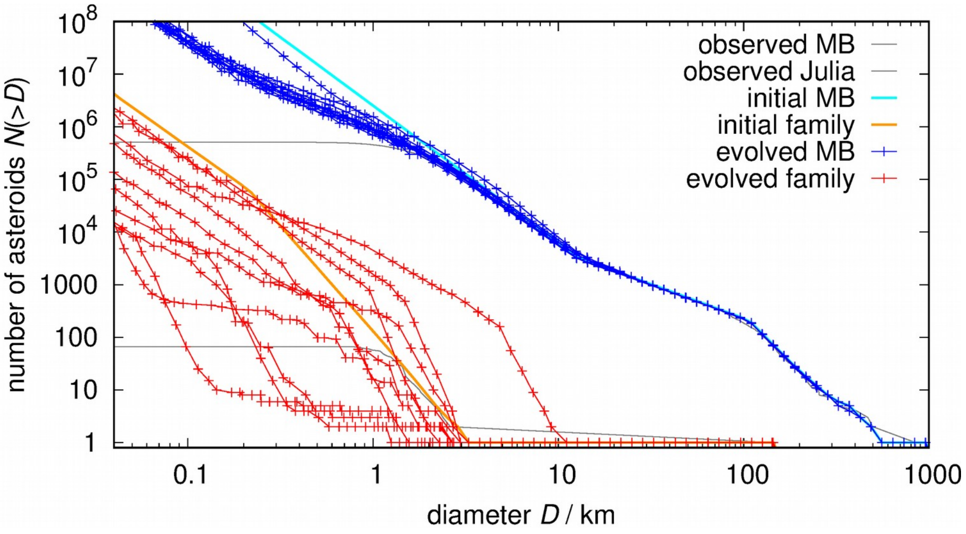

Crater size & position

- estimated crater size D = (74.8 ± 5.0) km (SPH: >60 km)
- **excavated** volume V_{ex} = (9800 ± 4900) km^3 (SPH: 7600 km^3)
- **ejected** volume V_{ej} = 176 km^3, i.e. $V_{ej} \ll V_{ex}$

- SPH: ejection velocity wrt. barycentre $v_{ej} \doteq 100$ m/s → $\Delta I = 0.002$ rad, cf.

$$\Delta I = \frac{\Delta v_W}{na\sqrt{1-e^2}} \frac{r}{a} \cos(\omega + f)$$

- **obliquity** of Julia γ = -17°; for $\varphi = \gamma$, ejecta can fly the most above (or below)
- Nonza with **latitude** φ = -32° is in a suitable position! (no spin evolution)

Conclusions

- 20 yr after HST observations of (4) Vesta…
- **asteroid families ↔ craters identifications** possible from ground-based observations!
- 40-m class telescopes (ELT) will be used

- Vernazza etal. (2018) A&A, **618**, A154